Instability in suspensions oscillating along narrow channels

Alejandro Adrián García^{1,2,a}, Yanina Lucrecia Roht^{1,b}, Georges Gauthier², Dominique Salin², German Drazer³, Jean-Pierre Hulin², and Irene Ippolito¹

^aaagarcia@fi.uba.ar ^byroht@fi.uba.ar

Abstract—The addition of solid particles to a fluid can change significantly the way it flows. This is important in several practical situations like landslides produced by heavy rain, waste treatment and blood flow. In some cases, the presence of solid particles has been shown to accelerate mixing in viscous flows through small channels. In this work, we show that oscillatory flow induces an instability characterized by particle motion transverse to the main flow, which could help improve mixing. We perform experiments with non-Brownian spherical particles (diameter 40 µm) suspended in a viscous fluid subject to squarewave oscillations inside a channel of rectangular cross-section (gap 1 mm, width 10 mm). Using fluorescence we visualize and track the particles in a plane across the gap and along the length. After a number of oscillations, we observe small but significant displacements of the particles across the gap. These displacement have oscillatory and long-term drift components, both spatially periodic along the flow direction. The latter may account for the transverse deformation of a high particle volume fraction region present in the center of the channel. Finally, we define and characterize an onset time for this instability as a function of the oscillation amplitude and the volume fraction.

Keywords—suspensions, particle tracking, oscillatory flow

I. INTRODUCTION

The use of small channels (micro- or millimeter scale) in chemical, pharmaceutical and biomedical applications is increasingly common, but one recurring problem is the mixing. Due to the small scale of the systems, the Reynolds numbers are usually small and flow is laminar. In this case, the mixing of a solute in the fluid is driven only by molecular diffusion, which is a slow process, and long channels are usually required to achieve adequate mixing. Different strategies employing oscillatory flows in small channels have been reported not only to improve mixing [1], but also to stretch long molecules [2], downsize chemical processes [3] and extend residence times [4].

Digital Object Identifier: (only for full papers, inserted by LACCEI). **ISSN, ISBN**: (to be inserted by LACCEI).

DO NOT REMOVE

Another possibility is the addition of solid particles suspended in the fluid, making a *suspension*. The presence of particles has been shown to increase the mass transfer significantly [5], but they can modify significantly the characteristics of the flow. The most obvious is the increase of the viscosity with the fraction of the total volume occupied by the particles, until a jamming fraction (55-62%) is reached and flow is impeded [6]. Additionally, a non-Newtonian behavior appears due to normal stress differences and can generate secondary flows that might improve the mass transport of a solute [7].

On the other hand, when the direction of the flow is reversed, transient changes occur in the local organization of the particles (microstructure), resulting in a lower viscosity until a steady state is reached again [8]. This is specially relevant for oscillatory flows, where a succession of reversals happen. Oscillatory flows of suspensions in Hele-Shaw cells has been shown to be unstable at low Reynolds numbers, with a modulation of the particle volume fraction along the flow direction visible as stripes [9]. Recently, we studied the motion of the particles during the onset of this instability using experiments with a model system composed of non-Brownian spherical particles and a Newtonian solution [10]. We found displacements of the particles across the cell gap (i.e. channel thickness), increasing the complexity of the flow, a characteristic usually sought to improve mixing in otherwise laminar flows.

In the present work, we extend those results by studying the connection between the long-term motion of the particles and the modulation of the particle volume fraction. Following a description of the experimental setup and the methods used, we present the results in four parts. First, a brief description of the initial state. Second, the growth with time of displacements transverse to the main flow and their spatial distribution. Then, we define an onset time and study its dependence on the oscillation amplitude and the particle volume fraction. Finally, we show the particles cumulative displacements after several oscillations and the simultaneous change in the particle distribution. We conclude with a discussion of the potential use

of the oscillation-induced transverse motions to improve the mixing of a solute and the perspectives for future work.

II. MATERIALS AND METHODS

A. Particles and fluid

We work with poly(methyl methacrylate) (PMMA) spherical particles of diameter $d=40\pm 2\,\mu\mathrm{m}$ suspended in an aqueous solution composed of 39.4% in weight (wt) of ammonium thiocyanate (NH₄SCN), 36.7 %wt of glycerin and 23.9 %wt of water [11], [12]. At room temperature (21°C), the solution has the same density ($\rho=1185\,\mathrm{Kg/m^3}$) as the spheres, preventing their sedimentation. The index of refraction (1.49) is also matched to obtain transparent suspensions. The measured viscosity of the solution is $\eta_0=7.6\,\mathrm{mPa}\,\mathrm{s}$. We use particle volume fractions ϕ between 25 and 40% (ϕ is the fraction of the total volume of the suspension corresponding to the particles).

To study the motion of the particles, we dye a small fraction ($\sim 1\%$) of them with rhodamine, a fluorescent dye. As a result, when illuminated by green laser light (wavelength $532\,\mathrm{nm}$), the dyed particles shine orange and can be seen inside the suspension. An alternative method is to dye with rhodamine the solution instead of the particles. Both methods require illumination by a sufficiently thin laser sheet as explained in section II-C. Unless stated otherwise, the reported results were obtained using the first method.

B. Channel and flow control

The suspension is made to flow through a transparent channel made by machining a slot inside a PMMA block and closing it with a PMMA plate. See Fig. 1a. The channel has a rectangular cross-section where the thickness (i.e. the gap) $H=1\pm0.05\,\mathrm{mm}$ is much smaller than the other two dimensions (width $W=11\pm0.5\,\mathrm{mm}$ and length $L=200\,\mathrm{mm}$).

Before the experiments, a 10 ml syringe is filled with the suspension, connected to the channel and attached to a computer-controlled syringe pump. The channel is completely saturated, with its length along the vertical direction to allow the evacuation of air bubbles. Then, the pump is switched to a second syringe of 1 ml, previously filled with suspension and also connected to the channel, to allow a fine control of the flow rate. The channel remained in a vertical position for most experiments, except a few ones in which it was set horizontally (gravity in the gap direction) and which provided similar results.

During the experiments, a symmetrical square-wave variation of the flow rate with maximum $Q_0=0.8\,\mathrm{ml/min}$ is used. Given the measured cross-section $S=11.5\,\mathrm{mm^2}$, the average absolute velocity is $V_0=Q_0/S\cong 1.16\,\mathrm{mm/s}$ and the Reynolds number is estimated as $\mathrm{Re}=V_0H\rho/\eta_0\cong 0.4$. Using oscillation periods T between 2 and $16\,\mathrm{s}$, we produce oscillatory displacements of the particles of average amplitude $A_0=V_0T/2$ between 1.2 and 9.7 mm, as sketched in Fig. 1b. No significant dependence of the results on the flow rate was found. Between experiments, the channel is drained and filled again to produce similar initial conditions.

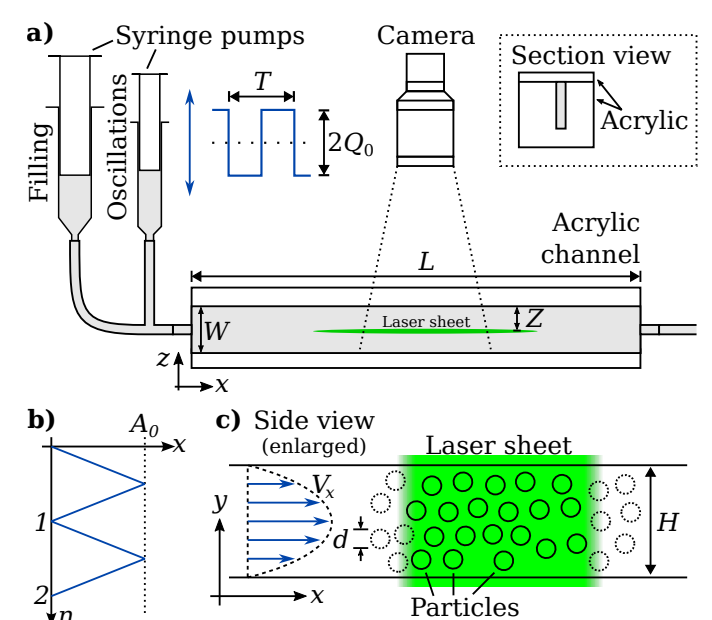


Fig. 1. Schematic of the experimental setup. a) View in the plane of the width and the length of the channel. The channel is connected to the two syringe pumps and observed by a camera from the side. The laser sheet comes from above and is shown as a green line in the center of channel. Top right: view of the cross-section showing that the channel is made of two acrylic parts. b) Sketch of the average oscillation displacements as a function of the number n of cycles. c) View in the thickness-length plane of the channel as seen during the experiments.

C. Visualization and data processing

The suspension inside the channel is illuminated with a laser sheet across the gap and along the length, situated in the middle of the width (z=W/2), as shown in green in Fig. 1 (a and c). This allows us to see only the particles inside this plane as explained before. The sheet is produced with a Gaussian laser beam and a Powell lens, with the addition of a spherical and a cylindrical lens to reduce the thickness down to $\sim 20 \, \mu m$, below the size of the particles.

Figure 2 shows typical images captured by the camera using both visualization methods. With the first method (top image), the dyed particles can be seen as white dots. The method is good to track and count the particles without much overlap, but the amount of information obtained may be limited to perform statistics, since not all particles are visible. On the other hand, with the second method (bottom image), the dye is in the fluid but the particles we use (Microbeads, CA40) adsorb the dye and shine as rings. A larger number of particles is visible and their tracking remains possible, but some overlap between particles may occur, making their precise counting trickier.

Images from experimental videos are processed to detect the particles. Each image is first convoluted against a pattern corresponding to one isolated particle, then, a threshold is used to remove background noise and finally, the positions of the centers of the particles are obtained by finding the local intensity maxima.

The position of the particles in consecutive images are compared and those spaced by less than one particle diameter

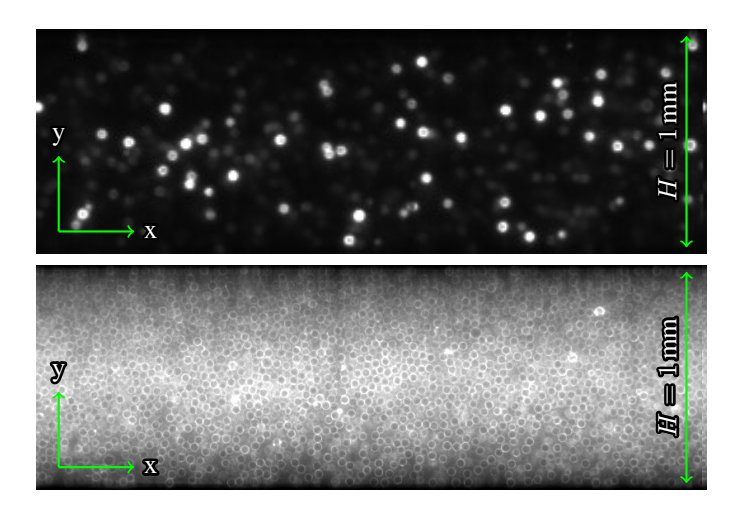


Fig. 2. Small regions ($\sim 3\,\mathrm{mm}$ by $H=1\,\mathrm{mm}$) of two example images showing the particles inside the channel. Produced by both visualization methods: a few dyed particles (top) and dyed fluid (bottom).

are considered to correspond to the displacement of a same particle. The video frame rate is adjusted to enable this procedure. Following this, particle trajectories can be obtained and instantaneous velocities are calculated from them.

III. RESULTS AND DISCUSSION

A. Initial state

At the beginning of each experiment, the particles oscillate back and forth along the longitudinal direction x as a result of the flow imposed by the syringe pump. To characterize this movement, we calculate longitudinal velocity profiles. First, the transverse direction y is divided into bins of equal size and the average particle velocity is calculated inside each one. Considering only the x component, we obtain instantaneous profiles $V_x(y,n)$, where n is the number of cycles. Then, we take the absolute value and average in time (i.e. n) during the first four cycles. Care is taken to exclude from the temporal averages a short time after each flow reversal, since the pump cannot induce an instantaneous change of the velocities. The resulting profiles $|V_x|(y)$ are shown in Fig. 3 for different particles volume fractions ϕ and normalized by the average value across the gap $\overline{V_x}$.

As the volume fraction ϕ increases, the profiles become increasingly blunted in the center. This a consequence of the shear-induced migration of particles from regions of high velocity gradient near the walls $(y/H=\pm 0.5)$ to regions of low one near the center (y/H=0), know to occur in pressure-driven flows [13], [14]. This migration produces a higher concentration of particles in the center than near the walls, which results in a nonuniform viscosity across the gap and the blunted velocity profiles. In our case, this process occurs mostly while the channel is being filled before each experiment.

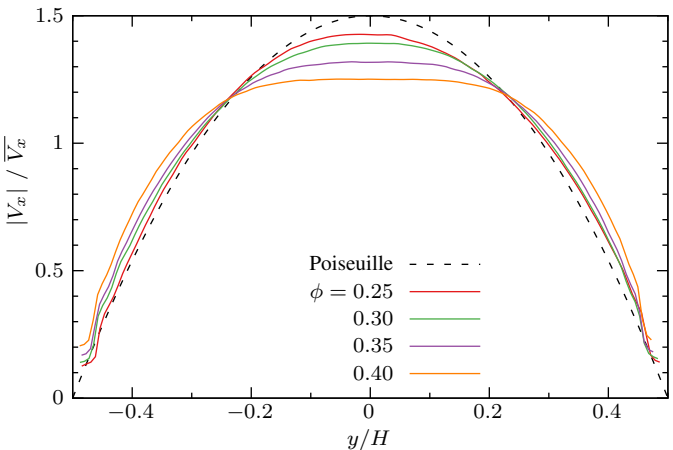


Fig. 3. Profiles across the gap of the absolute longitudinal velocity normalized by its average value and shown for different particle volume fractions ϕ . Oscillation amplitude $A_0/H=4.6$.

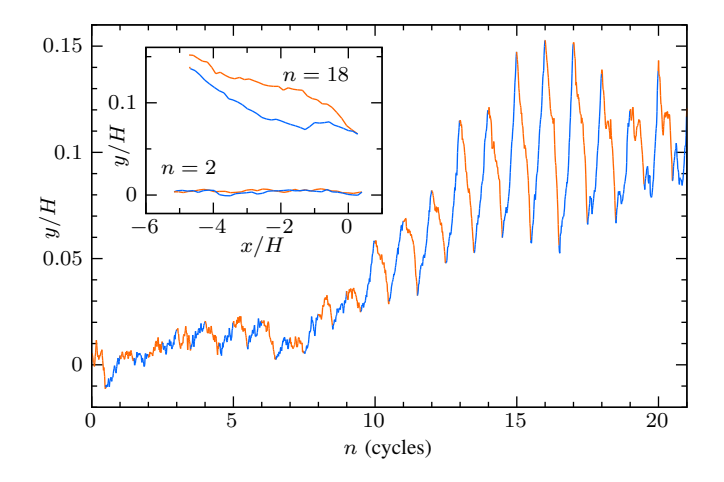


Fig. 4. Transverse position of an example particle for the duration of one experiment ($\phi=35\%$, $A_0/H=3.6$). The particle is always located near the center of the gap at y/H=0. Inset: trajectory of the same particle in the plane (x,y) during one oscillation cycle at the beginning and another one later in the experiment.

B. Transverse displacements

As mentioned before, near the walls $(y/H=\pm 0.5)$, the velocity gradient is large and nearby particles located at different transverse positions y move past each other, resulting in transverse displacements. On the other hand, near the center (y/H=0), the velocity gradient is small and the particles have minimal displacements along y.

After a number of oscillations, we observe that the particles begin to have larger transverse displacements, specially clear in the central band. As an example, Fig. 4 shows the coordinate y of an individual particle as a function of the number n of oscillations performed. Initially, there is only a slow drift, but after ≈ 10 oscillations, we see the onset of a transverse oscillatory motion with the same period and phase as the main oscillations along x. The inset of the figure shows the trajectory in the plane (x, y) during one oscillation cycle at the

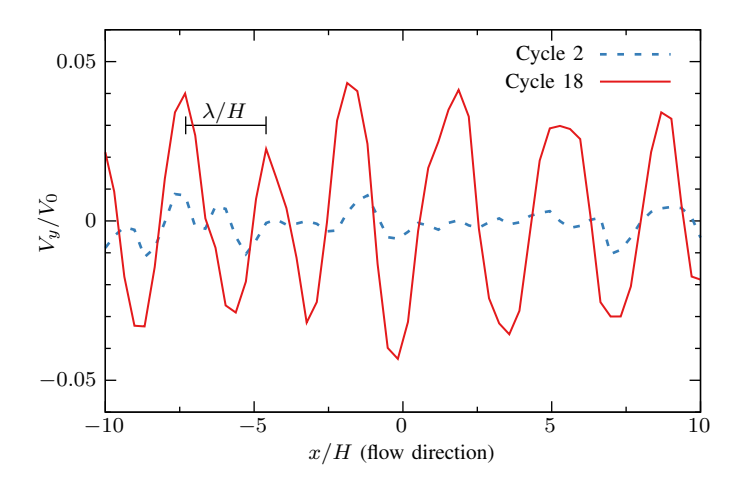


Fig. 5. Instantaneous transverse velocity profiles calculated from the velocity of the particles in the central band. Same experiment as in Fig. 4. The values are normalized by V_0 . Two different cycles are compared at times just before the change in flow direction.

beginning (n=2), and one near the end (n=18). Comparing them, we see again the increased displacement along y, but also that the trajectory becomes irreversible: the particle moves forward and backwards through different paths and exhibits a net displacement after one oscillation.

To study the spatiotemporal dependence of this phenomenon, we divide the central band (-0.1 < y/H < 0.1) into bins of equal size along the flow direction (x) and calculate the average of the velocities of the particles inside each bin. Taking only the y component of the velocity, we obtain instantaneous velocity profiles $V_y(x,n)$. Figure 5 shows the instantaneous results for two different cycles a short time before the change in flow direction. Comparing both cycles, one at the beginning and one after a number of oscillations, we see again the growth in magnitude of the transverse velocity V_y . Moreover, the variation along x is periodic so that one can define a wavelength $\lambda/H \sim 3.5$.

Finally, we can quantify the temporal evolution of this growth in the transverse velocity by calculating the root mean square (RMS) of $V_y(x,n)$ over x and then, taking the average of each cycle to remove the periodic modulation induced by the main oscillations. The result $V_y^{\rm rms}(n)$ is presented in Fig. 6. Initially, $V_y^{\rm rms}$ has a low base value and, around the tenth cycle, the value starts to grow until the $19^{\rm th}$ cycle and then, decreases slightly.

In this section, we have presented an unstable behavior driven by the oscillatory flow and characterized by the development of spatially and temporally periodic transverse velocities. In the following section we will study the influence of the amplitude of oscillation A_0/H and the particle volume fraction ϕ on the rate at which the instability develops.

C. Influence of the experimental parameters

From curves like the one in Fig. 6 (main), we calculate the number n_{50} of oscillations before $V_y^{\rm rms}$ reaches the midpoint between the initial value and the peak value. We consider

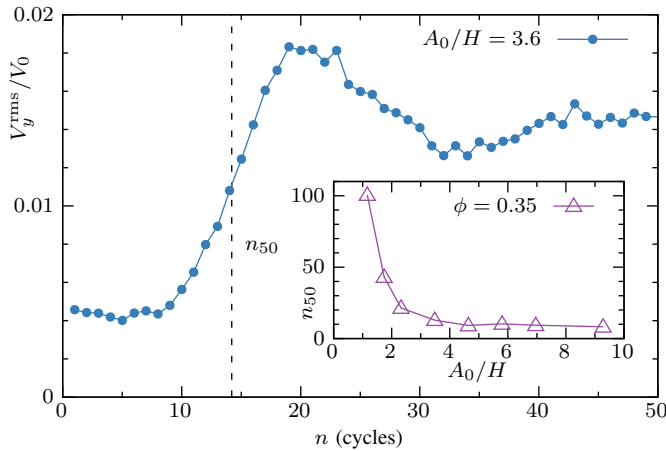


Fig. 6. Evolution with the number of oscillations of the RMS of the transverse velocities in the central band. Same experiment as in Figs. 4 and 5. The dashed vertical line marks the estimated number n_{50} of oscillations required to reach the midpoint between the initial and peak values. Inset: n_{50} for different oscillation amplitudes A_0/H , same $\phi=35\%$.

 n_{50} as the characteristic number of cycles before the onset of the instability and it can be fractional. The results for different oscillation amplitudes A_0/H are shown in the inset of the figure. It is clear that n_{50} sharply increases for low amplitudes, while the value remains more or less invariant for high amplitudes.

The inverse of n_{50} can be considered an estimation of the growth rate of the instability. Figure 7 shows $1/n_{50}$ as a function of the oscillation amplitude A_0/H and for different particle volume fractions ϕ . The growth rate increases monotonically with ϕ , suggesting that the instability is related to the particles encounters, since those become more frequent as ϕ increases [15]. Regarding the influence of A_0/H , we see again that $1/n_{50}$ is nearly constant for high amplitudes $(A_0/H \gtrsim 5)$, but in the lower limit, now it becomes evident that $1/n_{50}$ goes to zero as A_0/H approaches ~ 1 . We performed several long-duration experiments in an attempt to find any growth of V_y for $A_0/H < 1$ and $\phi = 40\%$ without any success, suggesting that the flow is stable below this threshold value.

The threshold for instability may be also associated with the particles encounters. A simple model is presented in [16] and [17] where particles need to move transverse to the main flow to prevent overlap between them when the suspension is deformed by the flow. For low enough oscillation amplitudes (this depends on ϕ) the particles can reach a so-called absorbing state, where they can move without colliding with each other. On the other hand, for higher amplitudes, this is impossible simply because there is not enough free space between the particles. Those results were reported for a uniform velocity gradient and it is not clear how to extend them for pressure-driven flows like the one studied here.

The constant number of oscillations required for the onset of the instability at high amplitudes, suggests a process that is only effective during a finite amount of time (or accumulated deformation) for each oscillation. Such a process could be

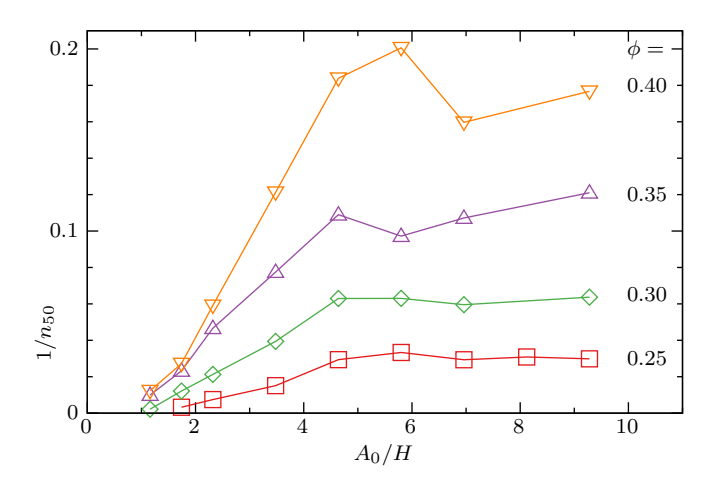


Fig. 7. Estimated instability growth rate for different oscillation amplitudes and particle volume fractions.

related to the particle reorganization that happens after flow reversal [18], [19]. Finally, the linear dependence between $1/n_{50}$ and A_0/H for $1 \lesssim A_0/H \lesssim 5$ can be related to the shear-induced diffusivity of particles (see a detailed discussion in [10]).

D. Irreversibility and particle migration

In addition to the oscillatory displacements, Fig. 4 shows an upward drift of the observed particle. Such drifts are a consequence of the irreversibility in the particles trajectories: the motion over both halves of the oscillation (forward and backward) do not cancel completely. Moreover, these net displacements are not random, like in a diffusive motion, but instead present some spatial periodicity, analogous to that previously shown for the instantaneous transverse velocity in Fig. 5. Figure 8 displays trajectories made taking only the positions of some particles at the beginning of each oscillation. Only the particles that could be tracked during four cycles or more where included. The colors blue and red mark the upward and downward trajectories, respectively. From this plot, we can conclude that at least a fraction of the particles present a spatially periodic long-term motion, with a wavelength between 3H and 4H.

The result of these irreversible displacements in the transverse direction (y) can be observed clearly in the experiments using the second visualization method (dyed fluid), as shown in Fig. 9. Initially (top image), there is a bright band along the flow direction (x) and in the center of the gap, due to the higher number of particles present there. This is a consequence of the shear-induced migration that occurs while the channel is filled before the experiment. Remember that the particles shine due to the adsorption of rhodamine from the fluid. After a number of oscillations, the particles start to move transverse to the main flow and the bright band deforms into the wavy pattern seen in the bottom image. The pattern is periodic along x, again with a wavelength between 3H and 4H.

In this section, we have seen the formation of a spatially periodic structure in the particle distribution as a consequence

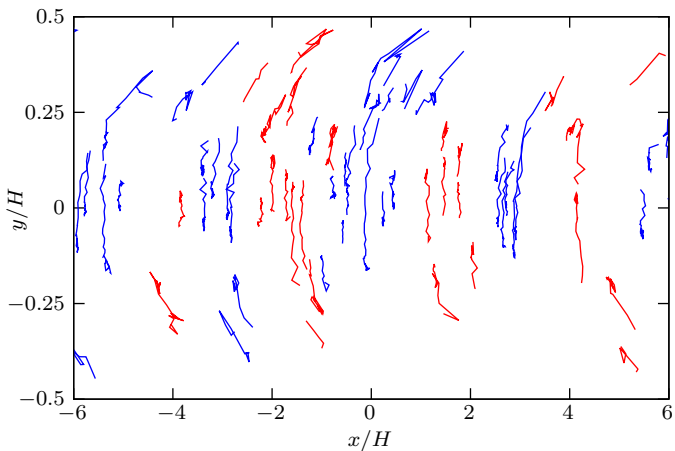


Fig. 8. Net displacements of some particles after each oscillation. Experiment with $A_0/H=2.4$ and $\phi=35\%$. The trajectories with a positive displacement along y are shown in blue, while in red for a negative one.

of irreversible transverse displacements induced by the oscillations. This structure is comparable with the one seen in images obtained by [9] using a similar experimental technique, but without the identification of individual particles.

IV. CONCLUDING REMARKS

We studied the behavior of solid particles suspended in a viscous fluid subject to an oscillatory flow along a narrow channel. We have shown the development of an instability characterized by the growth of particle displacements transverse to the main flow and spatially periodic along the flow direction. We define an onset time and show that it decreases with the particle volume fraction. Its dependence with the oscillation amplitude can be divided in three regimes. For low amplitudes $(A_0/H \lesssim 1)$, the flow is stable without any measurable growth in the transverse motions. For high amplitudes $(A_0/H \gtrsim 5)$, the number n_{50} of oscillation required for the onset remains approximately constant. Then, there is an intermediate regime where $1/n_{50}$ grows linearly with A_0/H .

Finally, we showed that these transverse motions have both an oscillatory component, with the same period as the main oscillations, and a long-term drift. This drift is an irreversible component in what would be otherwise a reversible motion where the particles retrace their previous trajectories after each flow reversal. Using a different visualization technique, we show that particle distribution, initially concentrated in the central band of the channel, changes into a wavy pattern at the onset of the instability, reflecting the spatial periodicity of the transverse motions.

The induction of a transverse flow component without the need of complex channel geometries might be useful to improve the mixing of both solvents and particles at low Reynolds numbers. In the future, we plan to test this hypothesis by studying the dispersion of a dye with an inhomogeneous initial distribution, and using both pure oscillatory flow and

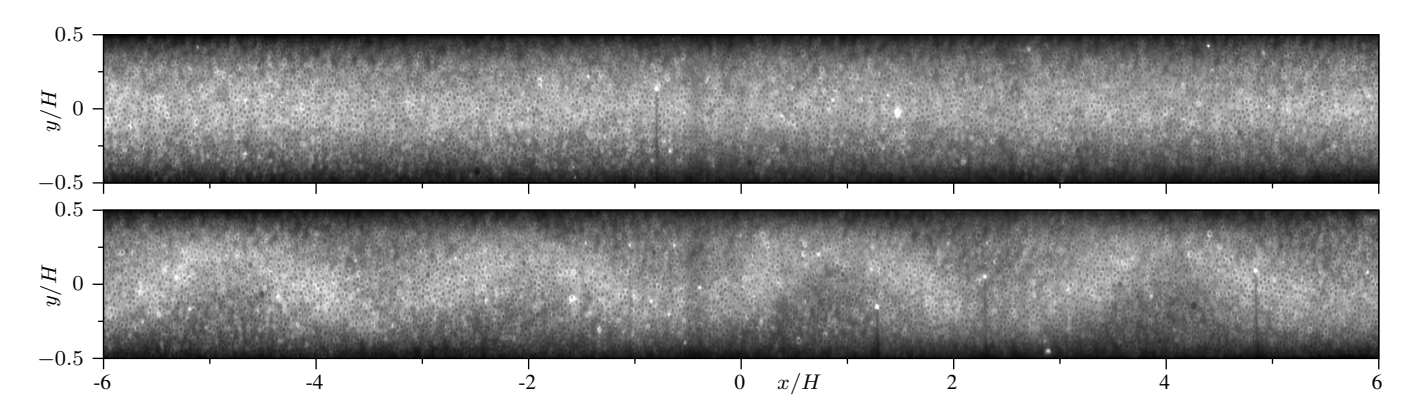


Fig. 9. Images taken at the start (top) and after 13 oscillations (bottom) of an experiment with the second visualization method (dye in the fluid). $\phi = 40\%$, $A_0/H = 3.6$.

oscillatory flow superimposed to a steady component, as would be required by some practical applications.

ACKNOWLEDGMENT

This work was funded by the research project UBACYT 20020170100225BA. During the course of this work, A. A. García was supported by a doctoral fellowship from the University of Buenos Aires and by the ADI program of the Paris-Saclay University.

REFERENCES

- [1] P. Tabeling, M. Chabert, A. Dodge, C. Jullien, and F. Okkels, "Chaotic mixing in cross-channel micromixers," *Philosophical Transactions of the Royal Society of London. Series A: Mathematical, Physical and Engineering Sciences*, vol. 362, no. 1818, pp. 987–1000, 2004.
- [2] K. Jo, Y.-L. Chen, J. J. de Pablo, and D. C. Schwartz, "Elongation and migration of single dna molecules in microchannels using oscillatory shear flows," *Lab Chip*, vol. 9, pp. 2348–2355, 2009.
- [3] G. Lestari, A. Salari, M. Abolhasani, and E. Kumacheva, "A microfluidic study of liquid–liquid extraction mediated by carbon dioxide," *Lab Chip*, vol. 16, pp. 2710–2718, 2016.
- [4] M. Abolhasani and K. F. Jensen, "Oscillatory multiphase flow strategy for chemistry and biology," *Lab on a Chip*, vol. 16, no. 15, pp. 2775– 2784, 2016.
- [5] M. Souzy, X. Yin, E. Villermaux, C. Abid, and B. Metzger, "Superdiffusion in sheared suspensions," *Physics of fluids*, vol. 27, no. 4, p. 041705, 2015.
- [6] E. Guazzelli and O. Pouliquen, "Rheology of dense granular suspensions," J. Fluid Mech., vol. 852, pp. 1–73, 2018.
- [7] A. Ramachandran, "Secondary convection due to second normal stress differences: A new mechanism for the mass transport of solutes in pressure-driven flows of concentrated, non-colloidal suspensions," *Soft matter*, vol. 9, no. 29, pp. 6824–6840, 2013.
- [8] F. Blanc, F. Peters, and E. Lemaire, "Local transient rheological behavior of concentrated suspensions," *Journal of Rheology*, vol. 55, no. 4, pp. 835–854, 2011.

- [9] Y. L. Roht, I. Ippolito, J. P. Hulin, D. Salin, and G. Gauthier, "Stripes instability of an oscillating non-brownian iso-dense suspension of spheres," *EPL*, vol. 121, no. 5, p. 54002, 2018.
- [10] A. A. Garcia, Y. L. Roht, G. Gauthier, D. Salin, G. Drazer, J. P. Hulin, and I. Ippolito, "Unstable oscillatory flow of non-brownian suspensions in hele-shaw cells," *Phys. Rev. Fluids*, vol. 8, p. 034301, Mar 2023.
- [11] B. C. Bailey and M. Yoda, "An aqueous low-viscosity density- and refractive index-matched suspension system," *Exp. Fluids*, vol. 35, no. 123, pp. 1–3, 2003.
- [12] D. Borrero-Echeverry and B. C. A. Morrison, "Aqueous ammonium thiocyanate solutions as refractive index-matching fluids with low density and viscosity," *Exp. Fluids*, vol. 57, no. 7, pp. 123–128, 2016.
- [13] M. K. Lyon and L. G. Leal, "An experimental study of the motion of concentrated suspensions in two-dimensional channel flow. part 1. monodisperse systems," *J. Fluid.Mech.*, vol. 363, pp. 25–56, 1998.
- [14] A. Rashedi, M. Sarabian, M. Firouznia, D. Roberts, G. Ovarlez, and S. Hormozi, "Shear-induced migration and axial development of particles in channel flows of non-brownian suspensions," *AIChE J.*, vol. 66, no. 12, p. e17100, 2020.
- [15] G. Drazer, J. Koplik, B. Khusid, and A. Acrivos, "Deterministic and stochastic behaviour of non-brownian spheres in sheared suspensions," *Journal of Fluid Mechanics*, vol. 460, pp. 307–335, 2002.
- [16] L. Corte, P. M. Chaikin, J. P. Gollub, and D. J. Pine, "Random organization in periodically driven systems," *Nature Physics*, vol. 4, no. 5, pp. 420–424, 2008.
- [17] P. Pham, J. E. Butler, and B. Metzger, "Origin of critical strain amplitude in periodically sheared suspensions," *Phys. Rev. Fluids*, vol. 1, p. 022201, Jun 2016.
- [18] J. M. Bricker and J. E. Butler, "Correlation between stresses and microstructure in concentrated suspensions of non-brownian spheres subject to unsteady shear flows," *Journal of rheology*, vol. 51, no. 4, pp. 735–759, 2007.
- [19] F. Peters, G. Ghigliotti, S. Gallier, F. Blanc, E. Lemaire, and L. Lobry, "Rheology of non-Brownian suspensions of rough frictional particles under shear reversal: A numerical study," *Journal of Rheology*, vol. 60, no. 4, pp. 715–732, Jul. 2016.